

CHAPTER 4 SOLUTION ALGORITHM

4.1 Numerical experiment

In this section, we demonstrate the feasibility and efficiency of the MLPG method through two numerical experiments with closed-form solutions.

The governing equation for solving the following two-dimensional time-dependent heat conduction equation subject to non-local boundary conditions in Ω , given by Abbasbandy (2010), can be written as:

$$\frac{\partial u}{\partial t} = \frac{\partial^2 u}{\partial x^2} + \frac{\partial^2 u}{\partial y^2}; \quad (x, y) \in \Omega \quad (4.1)$$

with initial condition

$$u(x, y, 0) = f(x, y), \quad \Omega = (x, y) \mid 0 \leq x, y \leq 1, \quad (4.2)$$

and boundary conditions

$$\frac{\partial u(0, y, t)}{\partial x} = g_0(y, t), \quad 0 \leq t \leq T, \quad 0 \leq y \leq 1, \quad (4.3)$$

$$\frac{\partial u(1, y, t)}{\partial x} = g_1(y, t), \quad 0 \leq t \leq T, \quad 0 \leq y \leq 1, \quad (4.4)$$

$$u(x, 1, t) = h_1(x, t), \quad 0 \leq t \leq T, \quad 0 \leq x \leq 1, \quad (4.5)$$

$$u(x, 0, t) = h_0(x)\mu(t), \quad 0 \leq t \leq T, \quad 0 \leq x \leq 1, \quad (4.6)$$

and the non-local boundary condition

$$\int_{\Omega} u(x, y, t) d\Omega = m(t), \quad 0 \leq x \leq 1, \quad 0 \leq y \leq 1, \quad (4.7)$$

where f , g_0 , g_1 , h_0 , h_1 and m are the given functions, while the functions u and μ are unknowns. The non-local boundary condition is variable-separable, with spatial dependence given by $h_0(x)$ and time dependence given by $\mu(t)$.

4.1.1 Numerical experiment I

In this implementation, we present two schemes for the first technique. The numerical solution in the first scheme uses a time step of $k + \frac{1}{2}$ with regular and irregular nodes and the second scheme uses a time step of $k + 1$ with regular nodes. For both schemes, we use the quadratic basis in the MLS approximations. The relative error is reported in the tables, defined as follows:

$$\|u\|_R = \sqrt{\frac{\sum_{i=1}^n (u_i - \hat{u}_i)^2}{\sum_{i=1}^n (u_i)^2}}$$

$$\|\mu\|_\infty = \max |\hat{\mu}_i - \mu_i|$$

To give a clear overview of our study, we have chosen the Mixed problem. So the numerical methods described in previous sections were applied to the following:

Mixed problem: For both schemes subject to non-local boundary conditions, we consider equation ((4.1)-(4.7)) with

$$f(x, y) = \exp(x + y), \quad g_0(y, t) = \exp(y + 2t), \quad g_1(y, t) = \exp(1 + y + 2t), \quad h_1(x, t) = \exp(1 + x + 2t), \quad h_0(x) = \exp(x), \quad m(t) = \exp(2t)(\exp(2) - 2\exp(1) + 1),$$

for which the exact solution is

$$u(x, y, t) = \exp(x + y + 2t), \quad \mu(t) = \exp(2t)$$

4.1.2 Numerical experiment II

In this implementation, we present two test problems with regular nodes and irregular nodes, to illustrate the efficiency and accuracy for the second technique. The calculations are performed with a local sub-domain size of 0.7 for each node of the

weight function, a local sub-domain size for each node of test function set to 0.6, and linear basis $m = 10$. The regularization parameter ε is chosen as $\varepsilon = 10^{-5}$.

We referenced two examples from Abbasbandy (2010) in a numerical scheme.

Example 1. For the first test problem with non-local boundary conditions, we consider equation ((4.1)-(4.7)) with

$$f(x, y) = \exp(x + y), \quad g_0(y, t) = \exp(y + 2t), \quad g_1(y, t) = \exp(1 + y + 2t), \quad h_1(x, t) = \exp(1 + x + 2t), \quad h_0(x) = \exp(x), \quad m(t) = \exp(2t)(\exp(2) - 2\exp(1) + 1),$$

for which the exact solution is

$$u(x, y, t) = \exp(x + y + 2t), \quad \mu(t) = \exp(2t)$$

Example 2. For the second test problem with non-local boundary conditions, we consider equation ((4.1)-(4.7)) with

$$f(x, y) = (1 + y)\exp(x), \quad g_0(y, t) = (1 + y)\exp(t), \quad g_1(y, t) = (1 + y)\exp(1 + t), \quad h_1(x, t) = 2\exp(x + t), \quad h_0(x) = \exp(x), \quad m(t) = \frac{3}{2}(\exp(1) - 1)\exp(t),$$

for which the exact solution is

$$u(x, y, t) = (1 + y)\exp(x + t), \quad \mu(t) = \exp(t)$$

4.2 Results

4.2.1 Results for numerical experiment I

Table 4.1 compares the results obtained for u and μ , between imposing only at Dirichlet boundary condition and imposing at Dirichlet boundary condition and Neumann boundary condition, at several time levels with $\Delta t = 0.1, T = 1$, on regular nodes in

Figure 4.1 ($N = 441$ nodes) from time step $k + \frac{1}{2}$.

Table 4.2 compares the results obtained for u and μ , between imposing only at Dirichlet boundary condition and imposing at Dirichlet boundary condition and Neumann boundary condition, at several time levels with $\Delta t = 0.1, T = 1$, on irregular nodes in

Figure 4.2 ($N = 121$ nodes) from time step $k + \frac{1}{2}$.

Table 4.3 compares the results obtained for u and μ , between imposing only at Dirichlet boundary condition and imposing at Dirichlet boundary condition and Neumann boundary condition, at several time levels with $\Delta t = 0.1$, $T = 1$, on regular nodes ($N = 441$ nodes) in Figure 4.1 from time step $k + 1$.

The numerical results show that the second scheme produces a higher accuracy than imposing only at Dirichlet boundary condition for mixed problem with regular nodes. The non-local integral boundary condition was discretized using Simpson's composite numerical integration rule, and the resulting discretized equation was approximated using MLS approximations. Our implementation has higher accuracy and is truly meshless.

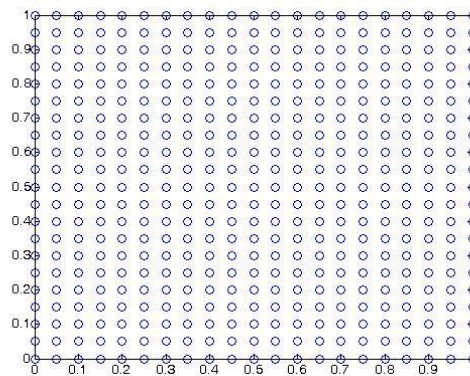


Figure 4.1 Regular nodes ($N = 441$ nodes) in the interval $[0,1] \times [0,1]$.

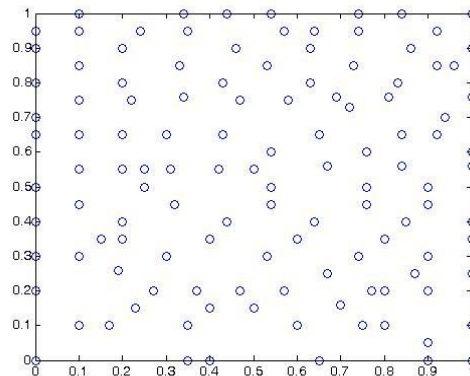


Figure 4.2 Irregular nodes ($N = 121$ nodes) in the interval $[0,1] \times [0,1]$.

Table 4.1 Relative error for heat conduction equation subject to non-local boundary conditions imposed only at Dirichlet boundary conditions, compared with imposing at Dirichlet and Neumann boundary conditions at time step $k + \frac{1}{2}$ with regular nodes $[21 \times 21]$.

t	Imposed at Dirichlet $r_0 \times 10^{-1}$	Imposed at Dirichlet and Neumann $r_0 \times 10^{-2}$	Imposed at Dirichlet $\ \mu\ _{\infty} \times 10^{-1}$	Imposed at Dirichlet and Neumann $\ \mu\ _{\infty} \times 10^{-1}$
0.1	1.2043	1.4851	5.2	0.8
0.2	0.8339	0.4881	3.3	0.2
0.3	1.0275	1.2276	6.2	1.0
0.4	0.8905	0.6393	5.8	0.4
0.5	0.9864	1.0950	8.7	1.4
0.6	0.9124	0.7212	9.1	0.8
0.7	0.9676	1.0162	12.4	1.9
0.8	0.9245	0.7736	13.9	1.4
0.9	0.9574	0.9671	18.3	2.6
1	0.9315	0.8082	21.1	2.3

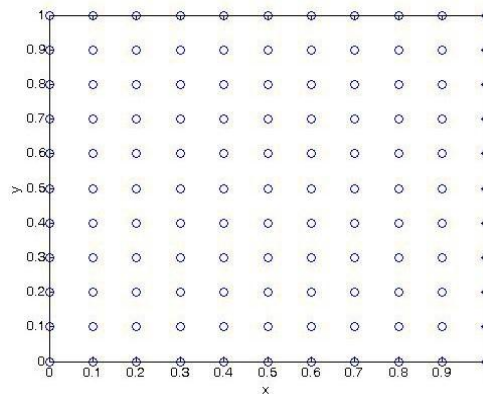


Figure 4.3 Regular nodes ($N = 121$ nodes) in the interval $[0,1] \times [0,1]$.

Table 4.2 Relative error for heat conduction equation subject to non-local boundary conditions imposed only at Dirichlet boundary conditions, compare with imposing at Dirichlet and Neumann boundary conditions at time step $k + \frac{1}{2}$ with irregular nodes [11×11].

t	Imposed at Dirichlet $r_0 \times 10^{-1}$	Imposed at Dirichlet and Neumann $r_0 \times 10^{-2}$	Imposed at Dirichlet $\ \mu\ _{\infty} \times 10^{-1}$	Imposed at Dirichlet and Neumann $\ \mu\ _{\infty} \times 10^{-1}$
0.1	1.3259	5.3081	7.9	0.8
0.2	0.7438	1.7463	5.1	0.2
0.3	1.0063	4.3908	8.5	1.1
0.4	0.8422	2.3207	8.8	0.4
0.5	0.9411	3.9321	12.1	1.4
0.6	0.8665	2.6106	13.5	0.8
0.7	0.9200	3.6561	17.7	1.9
0.8	0.8776	2.7891	20.4	1.4
0.9	0.9099	3.4811	26.1	2.7
1	0.8841	2.9063	30.7	2.3

Table 4.3 Relative error for heat conduction equation subject to non-local boundary conditions imposed only at Dirichlet boundary conditions, compared with imposing at Dirichlet and Neumann boundary conditions at time step $k + 1$ with regular nodes [21×21].

t	Imposed at Dirichlet $r_0 \times 10^{-1}$	Imposed at Dirichlet and Neumann $r_0 \times 10^{-3}$	Imposed at Dirichlet $\ \mu\ _{\infty} \times 10^{-1}$	Imposed at Dirichlet and Neumann $\ \mu\ _{\infty} \times 10^{-2}$
0.1	1.1885	2.3283	5.0	0.5
0.2	0.9000	2.6244	3.8	0.7
0.3	1.0249	2.4590	6.2	0.8

Table 4.3 Relative error for heat conduction equation subject to non-local boundary conditions imposed only at Dirichlet boundary conditions, compared with imposing at Dirichlet and Neumann boundary conditions at time step $k + 1$ with regular nodes $[21 \times 21]$ (continued).

t	Imposed at Dirichlet $r_0 \times 10^{-1}$	Imposed at Dirichlet and Neumann $r_0 \times 10^{-3}$	Imposed at Dirichlet $\ \mu\ _{\infty} \times 10^{-1}$	Imposed at Dirichlet and Neumann $\ \mu\ _{\infty} \times 10^{-2}$
0.4	0.9376	2.5495	6.3	1.1
0.5	0.9976	2.4950	8.8	1.2
0.6	0.9528	2.5296	9.8	1.6
0.7	0.9855	2.5066	12.8	1.9
0.8	0.9610	2.5222	14.8	2.3
0.9	0.9791	2.5114	18.9	2.8
1	0.9654	2.5190	22.3	3.4

4.2.2 Results for numerical experiment II

The efficiency and accuracy for the first test problem with regular nodes ($N = 121$ nodes), shown in Figure 4.3, are presented in Table 4.4, and those for the first test problem with irregular nodes ($N = 121$ nodes), shown in Figure 4.2, are presented in Table 4.5, at several time levels with $\Delta t = 0.1$, $T = 1$. Figure 4.4 and Figure 4.5 show the exact and approximate solutions. The efficiency and accuracy for the second test problem with regular nodes ($N = 121$ nodes) are presented in Table 4.6 and those for the second test problem with irregular nodes are presented in Table 4.7, at several time levels with $\Delta t = 0.1$, $T = 1$. Figure 4.6 and Figure 4.7 show the exact and approximate solutions. The relative error is reported in the tables.

The numerical results show that both test problems with regular nodes and irregular nodes give the same higher accuracy and efficiency.

Table 4.4 Relative error for heat conduction equation subject to non-local boundary condition on regular nodes $[11 \times 11]$ for Example 1.

t	$\ u\ _R$	$\ \mu\ _\infty$
0.1	4.8719×10^{-7}	4.0×10^{-4}
0.2	3.4257×10^{-7}	1.5×10^{-4}
0.3	4.2952×10^{-7}	3.2×10^{-4}
0.4	3.6685×10^{-7}	2.0×10^{-4}
0.5	4.0858×10^{-7}	2.8×10^{-4}
0.6	3.7830×10^{-7}	2.2×10^{-4}
0.7	3.9961×10^{-7}	2.7×10^{-4}
0.8	3.8394×10^{-7}	2.3×10^{-4}
0.9	3.9532×10^{-7}	2.6×10^{-4}
1	3.8684×10^{-7}	2.4×10^{-4}

Table 4.5 Relative error for heat conduction equation subject to non-local boundary condition on irregular nodes $[11 \times 11]$ for Example 1.

t	$\ u\ _R$	$\ \mu\ _\infty$
0.1	6.6513×10^{-7}	2.6×10^{-4}
0.2	3.3621×10^{-7}	2.6×10^{-5}
0.3	5.3451×10^{-7}	2.1×10^{-4}
0.4	3.8071×10^{-7}	7.0×10^{-5}
0.5	4.8523×10^{-7}	1.8×10^{-4}
0.6	4.0414×10^{-7}	9.6×10^{-5}
0.7	4.6244×10^{-7}	1.6×10^{-4}
0.8	4.1714×10^{-7}	1.1×10^{-4}
0.9	4.5074×10^{-7}	1.5×10^{-4}
1	4.2458×10^{-7}	1.2×10^{-4}

Table 4.6 Relative error for heat conduction equation subject to non-local boundary condition on regular nodes $[11 \times 11]$ for Example 2.

t	$\ u\ _R$	$\ \mu\ _\infty$
0.1	4.6999×10^{-8}	1.1×10^{-4}
0.2	3.7617×10^{-8}	6.9×10^{-5}
0.3	4.3393×10^{-8}	1.0×10^{-4}
0.4	3.9053×10^{-8}	7.7×10^{-5}
0.5	4.2191×10^{-8}	9.6×10^{-5}
0.6	3.9727×10^{-8}	8.1×10^{-5}
0.7	4.1620×10^{-8}	9.3×10^{-5}
0.8	4.0101×10^{-8}	8.4×10^{-5}
0.9	4.1306×10^{-8}	9.1×10^{-5}
1	4.0324×10^{-8}	8.5×10^{-5}

Table 4.7 Relative error for heat conduction equation subject to non-local boundary condition on irregular nodes $[11 \times 11]$ for Example 2.

t	$\ u\ _R$	$\ \mu\ _\infty$
0.1	2.0487×10^{-7}	2.3×10^{-4}
0.2	4.4914×10^{-8}	8.8×10^{-5}
0.3	1.5562×10^{-7}	2.0×10^{-4}
0.4	5.7379×10^{-8}	1.1×10^{-4}
0.5	1.3298×10^{-7}	1.8×10^{-4}
0.6	6.5350×10^{-8}	1.2×10^{-4}
0.7	1.1971×10^{-7}	1.7×10^{-4}
0.8	4.0101×10^{-8}	1.3×10^{-4}
0.9	1.1115×10^{-7}	1.6×10^{-4}
1	7.5281×10^{-7}	1.3×10^{-4}

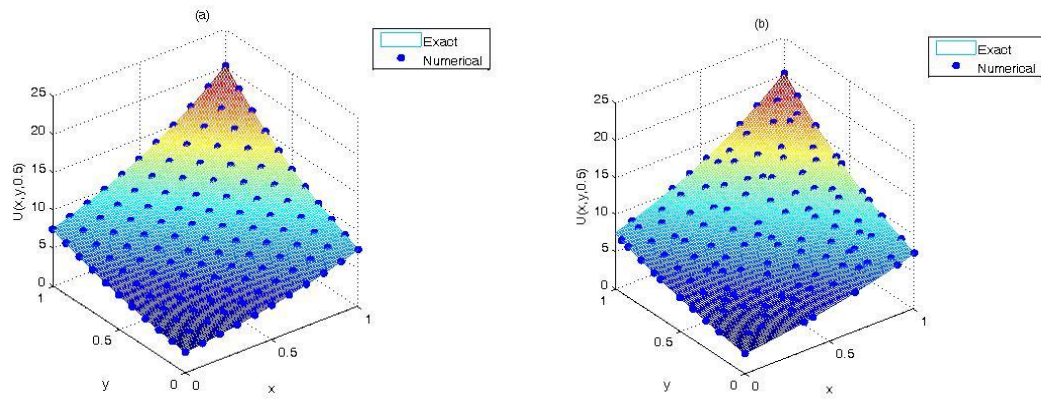


Figure 4.4 Exact and approximate solutions with regular (a) and irregular (b) nodes at $t = 0.5$ for Example 1.

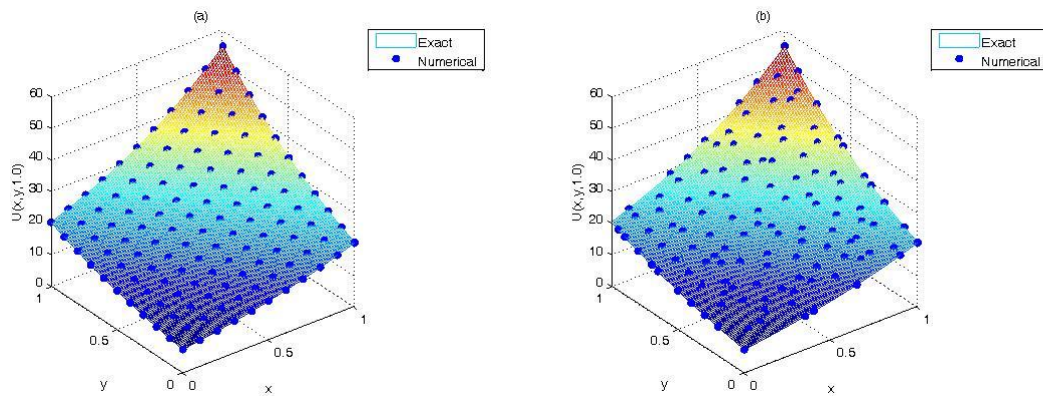


Figure 4.5 Exact and approximate solutions with regular (a) and irregular (b) nodes at $t = 1$ for Example 1.

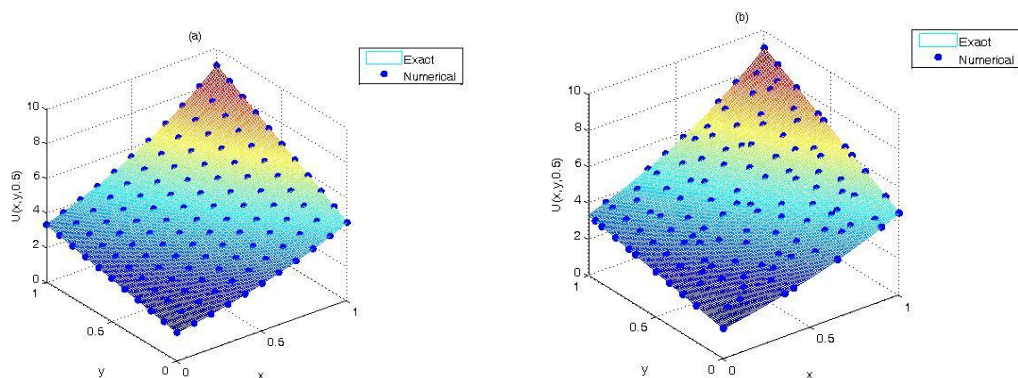


Figure 4.6 Exact and approximate solutions with regular (a) and irregular (b) nodes at $t = 0.5$ for Example 2.

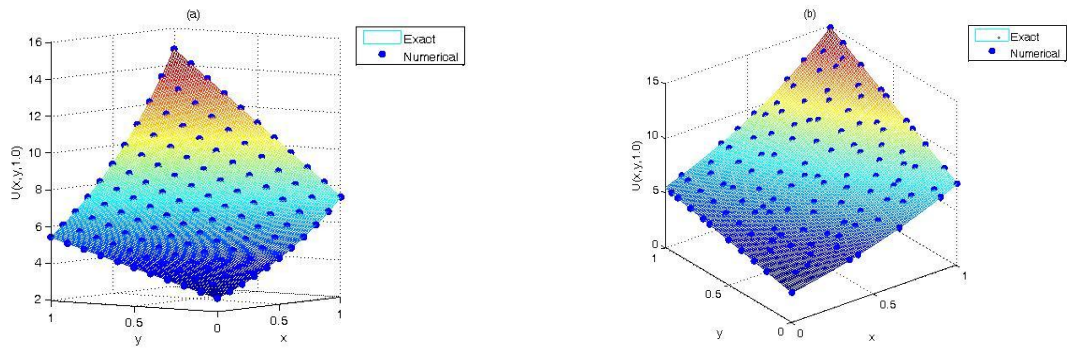


Figure 4.7 Exact and approximate solutions with regular (a) and irregular (b) nodes at $t = 1$ for Example 2.